Anal Bioanal Chem (2007) 389:2115–2124
DOI 10.1007/s00216-007-1599-y

ORIGINAL PAPER

Photonic crystal sensor for organophosphate nerve agents utilizing the organophosphorus hydrolase enzyme

Jeremy P. Walker · Kyle W. Kimble · Sanford A. Asher

Received: 9 July 2007 / Revised: 30 August 2007 / Accepted: 3 September 2007 / Published online: 27 September 2007

Abstract We developed an intelligent polymerized crystalline colloidal array (IPCCA) photonic crystal sensing material which reversibly senses the organophosphate compound methyl paraoxon at micromolar concentrations in aqueous solutions. A periodic array of colloidal particles is embedded in a poly-2-hydroxyethylacrylate hydrogel. The particle lattice spacing is such that the array Bragg-diffracts visible light. We utilize a bimodular sensing approach in which the enzyme organophosphorus hydrolase (OPH) catalyzes the hydrolysis of methyl paraoxon at basic pH, producing *p*-nitrophenolate, dimethylphosphate, and two protons. The protons lower the pH and create a steady-state pH gradient. Protonation of the phenolates attached to the hydrogel makes the free energy of mixing of the hydrogel less favorable, which causes the hydrogel to shrink. The IPCCA's lattice constant decreases, which blueshifts the diffracted light. The magnitude of the steady-state diffraction blueshift is proportional to the concentration of methyl paraoxon. The current detection limit is 0.2 μmol methyl paraoxon per liter.

Keywords Sensor · Pesticide · Organophosphate · Organophosphorus hydrolase · Enzyme · Polymerized Crystalline Colloidal Array (PCCA)

Introduction

Synthetic organophosphorus compounds (OPs), such as parathion and paraoxon, are widely used agriculturally in both the United States and worldwide as pesticides and insecticides [1]. These compounds are also structurally similar to chemical warfare agents (CWAs) such as sarin, soman and VX. OP compounds are commonly found in agricultural wastes at levels of between 1 and 10,000 parts per million [1]. These compounds are potent inhibitors of the enzyme acetylcholinesterase (AChE) because they prevent breakdown of the neurotransmitter acetylcholine at the neural synapse [2]. The inhibition of acetylcholine breakdown and subsequent accumulation results in a loss of muscular function and can result in paralysis or death if untreated [3, 4]. Due to the widespread use of these agents in agriculture, a high risk of food and groundwater contamination exists. The neurotoxicity of OP compounds is of immense concern, given their potential for use in chemical terrorism. Due to this threat, there is intense interest in developing sensors which can rapidly and selectively detect OP compounds for environmental analysis as well as for military/law enforcement applications such as counterterrorism and battlefield detection of OP agents. Rapid detection is a crucial element for preventive response, exposure treatment, and decontamination.

Several types of techniques exist for the detection and identification of OPs. Thin-layer chromatography, HPLC and GC/MS techniques are commonly used and provide nanomolar detection limits [5, 6]. These techniques are, however, expensive and time-consuming, requiring significant sample preparation and skilled technicians for their operation, which limits their practical use in field detection. Molecularly imprinted polymers (MIPs) which have very high selectivity towards OP substrates have also been developed. These sol-gel films utilize silanes, which are functionalized to create OP-binding templates. Detection of the sequestered OP molecules is achieved using fluorescence or electrochemistry [7].

J. P. Walker · K. W. Kimble · S. A. Asher (✉)
Department of Chemistry, Chevron Science Center,
University of Pittsburgh,
Pittsburgh, PA 15260, USA
e-mail: asher@pitt.edu

Recent research has focused on developing sensors which utilize biological recognition elements such as enzymes to detect and quantify OPs. These sensors provide a significant advantage over current chemical sensing techniques because they utilize specific enzymes which have very high affinities for OP analytes. For example, AChE and organophosphorus hydrolase (OPH, also called phosphotriesterase) have been extensively utilized in biosensor development.

AChE is inhibited by OPs at the catalytic serine site, which prevents turnover of acetylcholine at the neural synapse [2]. Several OP sensors utilize AChE either by using it directly to bind an OP and then measuring the sensor's response, or by measuring changes in the substrate turnover caused by exposure to OPs [8–12]. A flow injection technique has been developed in which AChE is immobilized onto a polymer substrate [8]. A sample solution containing OP is then exposed to the immobilized enzyme. A solution containing an enzyme substrate and a reagent which reacts to form a chromophore upon substrate catalysis is subsequently added. The absorbance of the chromophore is monitored to detect changes in enzyme activity caused by OP inihibition. Leon-Gonzalez and Townshend achieved 8-nmol OP/L OP detection limits with this technique [8].

Langmuir–Blodgett multilayer sensors have been developed that utilize AChE along with several other recognition elements. These sensors, which monitor changes in fluorescence caused by OP binding, also achieved nM detection limits [9, 10]. Amperometric sensors have also been fabricated which utilize AChE to detect very low OP concentrations [11]. These techniques can be easily miniaturized and are less expensive. Thus, they are more suitable for field detection than most other types of sensors. However, they are subject to interference from the other oxidizable substances present in real samples [11]. A piezoelectric sensor which monitors the binding of cholinesterase to inhibitors using a mass-sensitive quartz crystal was also recently developed. The sensor is capable of detecting 10^{-10} mol paraoxon/L [12].

We previously demonstrated a photonic crystal sensor which acts as a dosimeter and which operates in low ionic strength solution. The sensor detects OPs based on a change in the ionic free energy of the system due to the creation of a charged species that forms when parathion inhibits AChE [13]. The binding of OP shifts the wavelength of the visible light that is Bragg-diffracted by the PCCA. This sensor achieves unprecedented (femtomolar) detection limits; however, it only works in low-ionic strength solutions, and is therefore not ideally suited for use in real samples.

Sensors which utilize AChE are fundamentally limited in their development for two primary reasons. First, AChE can be irreversibly inhibited by several other species, such as carbamates and some neurotoxins [7]. These interferences could cause false positives for OP detection. Alternatively, they could cause false negatives by preventing OP binding to AChE altogether. Secondly, AChE is irreversibly inhibited by OPs, so sensors are not continuous or reusable, which increases the cost of performing the analysis. In light of these limitations, researchers have begun to explore the utility of other enzymes for OP detection.

Several researchers have utilized the recombinant enzyme organophosphorus hydrolase (OPH) instead. The development of this recombinant enzyme has facilitated the development of sensors which take advantage of this enzyme's unique properties. OPH is a ~35-kDa protein normally present as a homodimer. OPH contains a divalent metal ion cofactor (usually Zn^{2+} or Co^{2+}) which catalyzes the hydrolysis of OP esters at pH 8–10, releasing two protons in the process [14–16]. The enzyme is not subject to as much interference from other species as AChE, which can be inhibited by carbamates in addition to OPs. Another advantage of OPH is that it is a recombinant enzyme; researchers have altered the sequence of the enzyme through site-directed mutagenesis in order to produce OPH species which catalyze specific OP species more efficiently [17]. The catalytic reaction of OPH is illustrated in Scheme 1.

Several types of sensors which utilize OPH have been developed. Potentiometric sensors based on measuring the pH changes caused by the OPH-catalyzed degradation of OP species have been developed [16, 18, 19]. For example, Mulchandani et al. reported a 2-μmol OP/L detection limit with one such system [16]. Amperometric sensors utilizing OPH have also been developed [20–23]. These sensors oxidize *p*-nitrophenol, a paraoxon hydrolysis product, which is then detected at a carbon paste electrode. Detection limits as low as 20 nmol paraoxon/L have been demonstrated [21]. Another sensor employed a bacterium

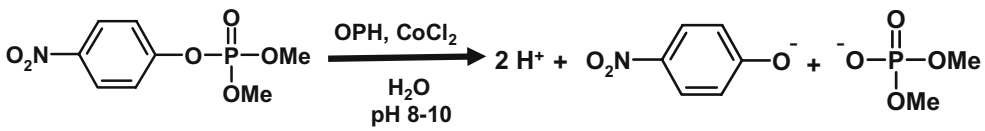

Scheme 1 OPH hydrolyzes methyl paraoxon, an organophosphorus pesticide, into *p*-nitrophenolate and dimethylphosphate at basic pH, producing two protons in the process

which oxidizes 2-nitrophenol to CO_2, consuming O_2 in the process. The O_2 consumed, which is measured by an oxygen electrode, correlates with the concentration of OP present. The detection limit for this technique was reported to be 0.2 μM OP [23].

OPH has also been recently utilized not only for sensing applications, but also for the decontamination of OP-containing samples [24, 25]. Current chemistry-based decontamination techniques frequently require the use of caustic materials; however, these strong alkalis can damage the contaminated objects as well as the environment [25]. OPH can eliminate the need to use caustics because it selectively hydrolyzes OP species. The possibility of producing multiuse reversible enzymatic systems capable of OP detection and decontamination would provide a significant advantage for anti-terrorism preparedness and for contaminant clean-up. Such systems would provide a rapid, cost-effective single approach to initial detection, decontamination, and the monitoring of the decontamination process.

We demonstrate in this paper the development of a novel, inexpensive sensor for the detection of OP species based on our previously developed intelligent polymerized crystalline colloidal array (IPCCA) photonic crystal sensing materials. These IPCCAs utilize an array of colloidal particles [26–31] polymerized into a hydrogel [32–35] network which Bragg-diffracts light in the visible spectral region. We utilize our recently developed general bimodular sensing motif that was originally demonstrated for sensing creatinine [36]. The first sensing element is an enzyme which reacts with the analyte to produce a steady-state pH gradient inside the hydrogel. The pH change is then detected by the second sensing element, which titrates to cause a sensing response.

Our OP-sensing IPCCA contains OPH, which degrades the OP methyl paraoxon to *p*-nitrophenolate and dimethylphosphate at pH 9.7, producing two protons. These protons protonate the secondary sensing element, 3-aminophenolate (3-AMP), causing a steady-state volume change in the PCCA. The wavelength of diffracted light shifts in response to the steady-state volume change of the hydrogel. Figure 1 illustrates this sensing motif.

Our PCCA sensor platform relies upon a volume phase transition phenomenon which occurs in the hydrogel matrix

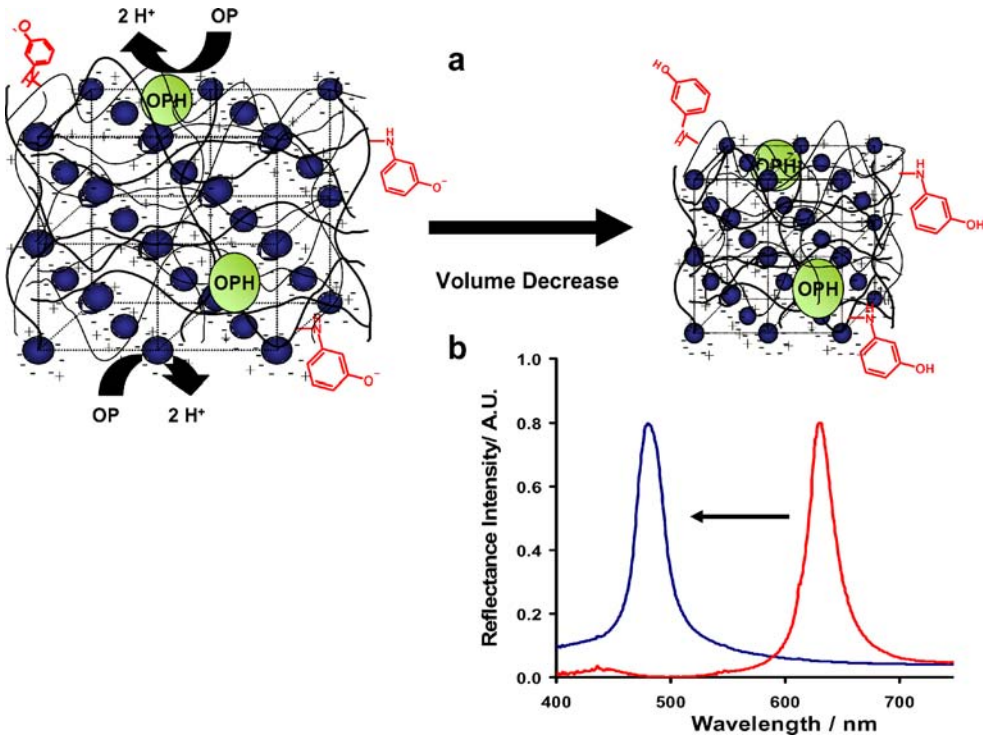

Fig. 1 **a** CCAs form due to electrostatic repulsion between particles. The particle spacing is such that the array Bragg-diffracts visible light. The lattice is locked into place by a poly-2-hydroxyethylacrylate hydrogel network. The backbone is functionalized with both organophosphorus hydrolase (OPH) and 3-aminophenolate. As OPH reacts with methyl paraoxon, *p*-nitrophenolate and dimethylphosphate, as well as two protons, are produced. This produces a steady-state pH gradient between the interior and exterior regions of the hydrogel. The lower pH inside the hydrogel protonates the phenolates. As a result, the solubility of the hydrogel network decreases, which shrinks the hydrogel and blueshifts the IPCCA diffraction. **b** The diffraction peak of the IPCCA blueshifts in response to increasing analyte concentration

due to changes in the free energy of the system. For this sensor, the volume change is caused by a change in the free energy of mixing (ΔG_{mix}) of the hydrogel [37]. The back-diffracted light follows Bragg's Law:

$$\lambda_0 = 2\ n\ d \sin\ \theta$$

The wavelength (λ_o) of the light diffracted by the IPCCA's 111 plane of the fcc lattice depends upon the plane spacing (d), the refractive index (n) of the system, and the Bragg glancing angle, θ. Because we are sampling normally incident light, sinθ is unity. We demonstrate that our sensor reversibly detects the OP pesticide methyl paraoxon at sub-micromol/L concentration levels in lab buffer solution as well as in streamwater samples. This work provides proof-of-concept that the sensor could be practically implemented as part of a device for the continuous monitoring of OP pesticides or nerve agents.

Experimental

PCCA preparation

Figure 2 depicts the synthesis and functionalization of the OP IPCCA sensor. 2-Hydroxyethylacrylate (2-HEA, 0.94 g, 8.1 mmol, Sigma, St. Louis, MO, USA), acrylamide (AMD, 0.02 g, 0.28 mmol, Fluka, Buchs, Switzerland), polyethylene glycol (200) dimethacrylate (PEGDMA-200, 0.09 g, 0.25 mmol, Polysciences, Warrington, PA, USA), glycidyl acrylate (GA, 0.04 g, 0.37 mmol, Sigma) and ethylene glycol (1.95 g, 31 mmol, J.T. Baker, Phillipsburg, NJ, USA) were mixed and treated with Al_2O_3 to remove inhibitors from the monomers. The mixture was centrifuged to separate the monomer from the Al_2O_3. 1.015 g of this solution was mixed with the colloid suspension (1.0 g, 5–10% m/m dispersion, polystyrene latex spheres, 120 nm) [26–31]. AG501-X8 (D) ion exchange resin (~0.1 g, 20–50 mesh, mixed bed, Bio-Rad, Hercules, CA, USA) and 10% diethoxyacetophenone (DEAP, 10 μL, 4 μmol, Aldrich, Milwaukee, WI, USA) in dimethylsulfoxide (DMSO, J.T. Baker) were mixed into the suspension in a 2-dr vial. After 15 min, the mixture was centrifuged to remove the ion-exchange resin and was injected between two quartz discs separated by a 125 μm-thick Parafilm spacer. The colloidal particles self-assemble into a crystalline colloidal array (CCA), resulting in a liquid film which diffracts light. The film was exposed to λ=365 nm UV light from mercury lamps (Blak Ray) for 3 h. A poly-2-HEA/AMD hydrogel network with PEGDMA crosslinks forms around the CCA, resulting in a polymerized CCA (PCCA) [32–35]. The

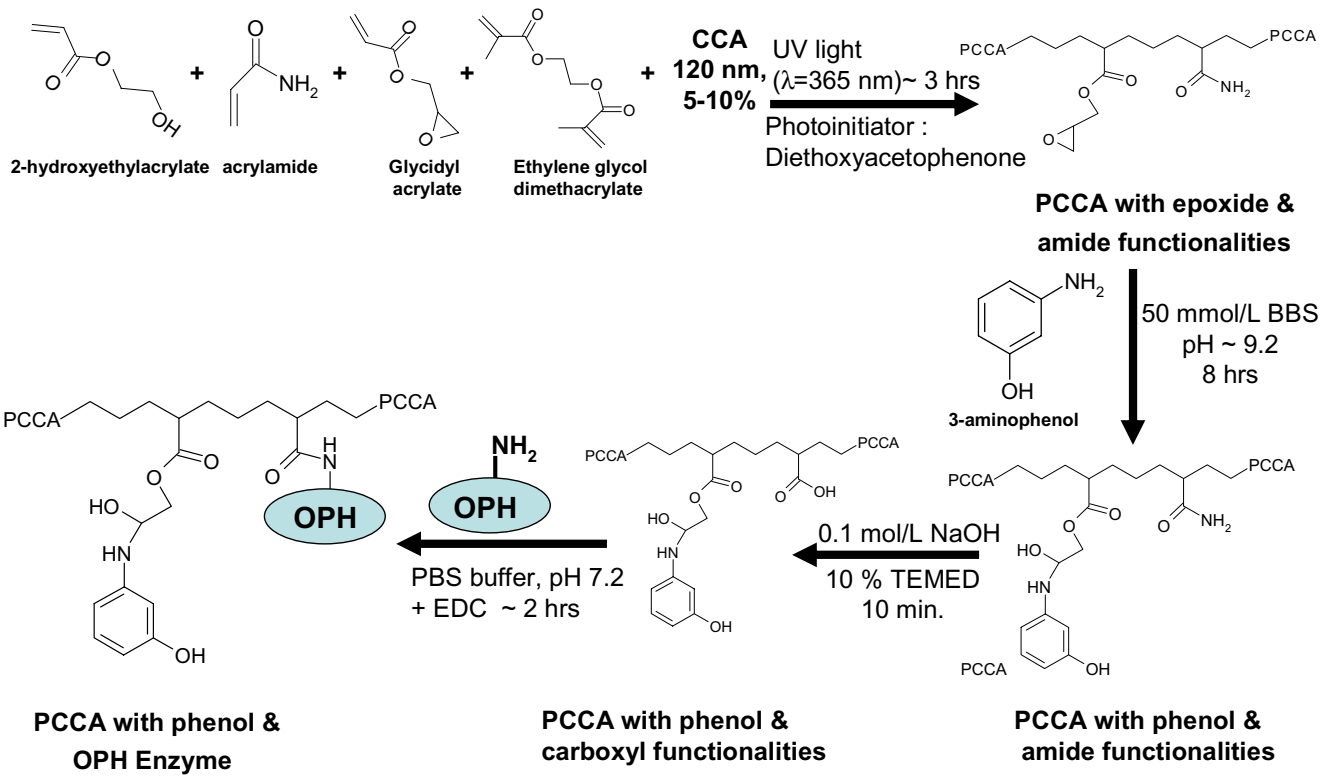

Fig. 2 Preparation of the IPCCA and functionalization with 3-aminophenol and OPH. The 3-AMP is first coupled via epoxide ring opening. The pendant amides are subsequently hydrolyzed to form carboxylates, which are carbodiimide-coupled to amines on the OPH enzyme

quartz cell enclosing the hydrogel was opened in nanopure water and the PCCA was allowed to equilibrate with water.

Attachment of 3-aminophenol

The PCCA was placed into a 50 mmol/L borate buffer solution (BBS, pH 9.2, J.T. Baker) to equilibrate before coupling. 0.5 g of 3-aminophenol (3-AMP, 4.6 mmol, Sigma) were dissolved in 10 ml DMSO (J.T. Baker) and then diluted to 50 ml with 50 mmol/L BBS. The solution and PCCA were placed in a 125-ml plastic container (Nalgene, Rochester, NY, USA) and allowed to react for 8 h. After reacting, the PCCA was rinsed hourly for 6 h with BBS. A blank gel (hydrogel without CCA) was prepared and functionalized according to the above protocol. UV-VIS spectra of the blank gel were measured by a Varian (Palo Alto, CA, USA) Cary 5000 UV-VIS spectrophotometer to confirm the attachment of 3-AMP by monitoring the absorbance at λ=290 nm. The sensor typically contains a 13 mmol/L concentration of 3-AMP.

Attachment of organophosphorus hydrolase

The PCCA was then hydrolyzed in a 50 mL solution of NaOH (0.1 mol/L, J.T. Baker) containing 10% v/v N,N,N′,N′-tetramethylethylenediamine (TEMED, Aldrich) for 10 min. The hydrolyzed PCCA was washed for 2 h with 150 mM NaCl (J.T. Baker). UV-VIS spectra were recorded to confirm that phenols remained attached to the hydrogel after hydrolysis.

A piece of the PCCA (1 cm ×1 cm ×125 μm) was allowed to adhere to a plastic petri dish (Falcon, BD Biosciences, San Jose, CA, USA). A coupling solution of enzyme was made by dissolving 6 mg organophosphorus hydrolase (OPH, EC 3.1.8.1., 6 mg solid, MW 35,000, Lybradyn, Inc., Oak Brook, IL, USA) in 200 μL of 0.1 mol/L phosphate buffer (PBS, Pierce Biotechnology, Rockford, IL, USA). The PCCA was incubated overnight in the enzyme solution to allow the OPH to diffuse into the hydrogel. Next, 0.1 g of 1-ethyl-3-(3-dimethylaminopropyl) carbodiimide hydrochloride (EDC, 0.52 mmol, Pierce Biotechnology) was dissolved in 100 μL of 0.1 mol/L 2-(N-morpholino)ethanesulfonic acid (MES, pH 4.7, Pierce Biotechnology). The EDC solution was added, and the reaction was allowed to proceed for 2 h. The sensor was rinsed in 150 mmol NaCl /L (J.T. Baker) and stored overnight until testing in 0.1 mol PBS/L solution at 4 °C. UV-VIS spectra were also recorded for a blank hydrogel treated in exactly the same way. OPH attachment was confirmed by monitoring the absorption difference spectrum of the blank hydrogel functionalized with 4-amino-2-nitrophenol instead of 3-AMP. The absorption difference spectrum was generated by subtracting spectra of the sample before and after coupling.

Solutions and diffraction measurements

The PCCA was stored in 0.1 mol PBS/L (pH 7.4) at 4 °C at all times when not being tested. We made a buffer test solution (BTS) which contained 2 mmol $Na_2B_4O_7{\cdot}10\ H_2O$/L (J.T. Baker), 5% v/v methanol (Fisher, Pittsburgh, PA, USA), 0.05 mmol $CoCl_2{\cdot}6H_2O$/L (Fisher), and 150 mmol NaCl/L (J.T. Baker). The test solution pH was adjusted to ~9.7 with 0.1 mol NaOH/L (Fisher).

The PCCA diffraction was monitored using a fiber-optic diode spectrometer with a tungsten halogen light source (Ocean Optics, Dunedin, FL, USA) using a reflectance probe. All measurements were conducted with the PCCA adhering to the bottom of the petri dish and with stirring using a magnetic stir bar.

The sensor was first titrated to confirm that the 3-AMP was attached and that the sensor responded to titration of the attached phenols with 20 mmol NaOH/L (Fisher). We used these data to confirm the pK_a values of the attached phenols.

We then tested the sensor with a control as well as in a series of BTS dilutions of the OP pesticide methyl paraoxon (ChemService, Inc., West Chester, PA, USA) ranging in concentration from 2.4 μmol/L to 1 mmol/L. The IPCCA was pre-equilibrated in BTS for 30 min prior to exposure to the methyl paraoxon solutions. Diffraction spectra were recorded until the diffraction stopped shifting, indicating that the sensor had reached steady-state. Responses were typically saturated in about 50 min. The sensor was subsequently rinsed and re-equilibrated in BTS. The sensor was subsequently exposed to a new methyl paraoxon solution. Two sensing runs were performed with the sensor on consecutive days. We utilized concentrations of 0–24 μmol methyl paraoxon/L to calculate the detection limit.

We also performed several control experiments in order to confirm that the response was due to a change in the free energy of mixing of the PCCA. We tested the sensor with various components absent in order to prove that the sensing response resulted from titration of the pendant phenolates by the protons produced during the OPH hydrolysis of methyl paraoxon. Several control studies were also performed to confirm the hypothesis that the sensor displays a steady-state response and not an equilibrium response.

Finally, the response of the sensor was tested in streamwater to determine the sensor performance in a real sample matrix. Water samples were obtained in July, 2006 from a small stream behind the Plantations housing development in Saxonburg, PA, USA. The sample was first filtered through a 2-μm filter to remove particulate matter. Then the streamwater samples were prepared by adding 5% (v/v) methanol to help solubilize the OP, 150 mmol NaCl/L,

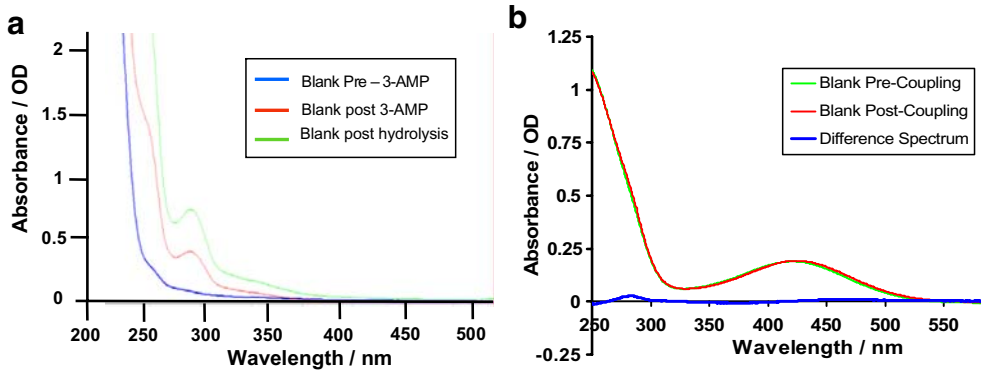

Fig. 3 UV-VIS absorbance spectra of CCA-free hydrogels. **a** The spectra at various stages of 3-AMP coupling. The *blue line* is the spectrum of a blank poly-2-HEA hydrogel prior to conjugation, the *green spectrum* is the blank after coupling with 3-AMP, and the *red spectrum* is obtained after hydrolysis and rinsing. **b** The spectra of a poly-2-HEA hydrogel with 4-amino-2-nitrophenol attached before (*green*) and after (*red*) OPH coupling. The *blue difference spectrum* represents the absorbance difference after coupling OPH. The peak at λ=280 nm in the difference spectrum indicates OPH attachment. 4-amino-2-nitrophenol, which absorbs at λ=430 nm instead of λ=280 nm, was coupled instead of 3-AMP in order to avoid extensive overlap between the absorbance peaks of 3-AMP and OPH

0.05 mmol $CoCl_2 \cdot 6H_2O$/L, 2 mmol $Na_2B_4O_7 \cdot 10\ H_2O$/L, and the pH was adjusted to 9.7 with 0.1 mol NaOH/L. This solution was used in place of the BTS to make serial dilutions of methyl paraoxon via the protocol used previously.

Results and discussion

UV-VIS confirmation of sensing element attachment

The conjugation of 3-AMP and OPH to the hydrogel matrix was monitored on a colloid-free hydrogel (blank gel) through absorption spectroscopy (Fig. 3). Each sensor was rinsed for several hours with 150 mmol NaCl/L solutions to remove unreacted species. The 3-AMP is initially present at a concentration of ~25 mmol/L, but the hydrolysis step necessary for coupling OPH also hydrolyzes some of the ester bonds between the phenolate and the hydrogel, leaving ~13 mmol phenol/L attached to the hydrogel (Fig. 3a). OPH attachment to a blank hydrogel was confirmed by monitoring the tyrosine/tryptophan absorbance at λ=280 nm. Prior to OPH coupling, 4-amino-2-nitrophenol, which does not have an absorbance maximum at λ=280 nm, was attached to the blank hydrogel instead of 3-AMP. Spectral overlap between OPH and 3-AMP was thus avoided. Figure 3b displays the difference spectrum of the blank hydrogel before and after OPH coupling. Using the extinction coefficient of the OPH monomer, 26,740 $M^{-1}cm^{-1}$ at λ=280 nm [38], we calculated an 8-μmol OPH/L concentration in the hydrogel using the difference spectrum.

We also proved that OPH was attached to the sensor by monitoring the λ=412 nm absorbance of *p*-nitrophenol, an OP hydrolysis product, in BTS containing methyl paraoxon, and found that the rate of hydrolysis was ~400 times greater in the presence of an OPH-functionalized PCCA than in the presence of a PCCA lacking OPH. The OPH hydrolysis rates are typically 40–2450 times faster than in a 0.1 mol NaOH/L solution [39]. This result also demonstrates that functional OPH is attached to the PCCA.

PCCA titration in test buffer

We monitored the diffraction of the PCCA with 3-AMP attached in BTS in order to determine the pK_a of the phenol groups, which should be close to the pK_a of 3-acetamidophenol (Fig. 4). Both the borate buffer (pK_a=9.2) and the 3-acetamidophenol (pK_a=9.65) groups titrate at their expected pK_a values [40]. We observed that when the pH rises above the inflection point of the buffer, the sensor diffraction wavelength shifts. We conclude that the response is due to the deprotonation of the phenols, which makes the free energy of mixing of the hydrogel more favorable [37]. The titration and diffraction measurements show inflection points at pH~9.6, the pK_a of the conjugated phenol. These measurements were repeated on the same PCCA after rinsing to demonstrate the reproducibility and reversibility of the response.

Dependence of PCCA diffraction on methyl paraoxon concentration

Our IPCCA organophosphate sensor contains both 3-aminophenol and OPH, which catalyzes the hydrolysis of methyl paraoxon and releases protons [16]. The products, *p*-nitrophenol and dimethyl hydrogen phosphate, have pK_a

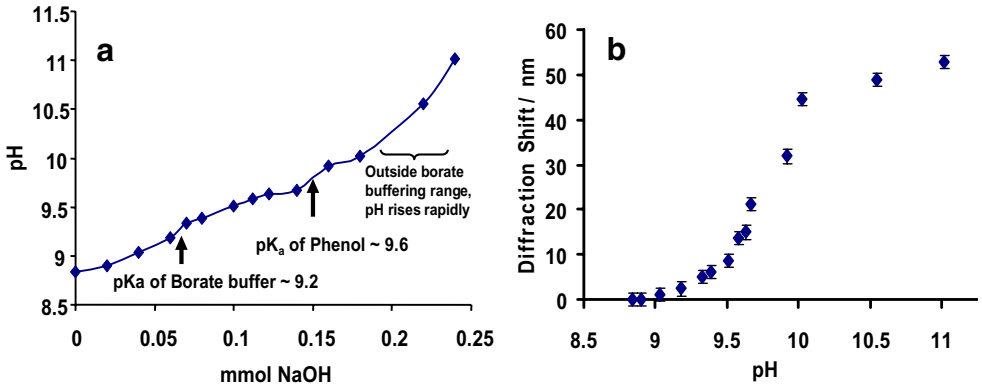

Fig. 4 **a** The solution pH versus the number of millimoles of NaOH added. The pK_a of the borate buffer (pH~9.2) and the 3-AMP (pH~9.6) are apparent. **b** Diffraction redshift of the PCCA as a function of the pH. From the graphs, we see that during the titration of the buffer there is very little response from the PCCA. However, as the phenol groups are titrated, we see that the PCCA diffraction redshifts. The inflection point in **b** occurs at the phenolate pK_a, indicating that the diffraction response is due to the phenol titration

values which are lower than the buffered solution pH of 9.2 (7.22 and 1.24, respectively) [40] and thus release their protons, which decrease the internal pH of the IPCCA and protonate the pendant phenolates. This causes a steady-state reduction in the free energy of mixing, causing the gel to shrink. This volume change blueshifts the diffraction in proportion to the concentration of methyl paraoxon.

Figure 5 shows the methyl paraoxon concentration dependence of our IPCCA sensor diffraction in BTS. The diffraction wavelength blueshifts with increasing concentration of methyl paraoxon. The shift essentially saturates by 240 μmol methyl paraoxon /L. At lower concentrations (≤24 μmol/L) the response is quite linear, so a detection limit can be calculated. This concentration range is shown in the inset of Fig. 5a. The detection limit is determined by the concentration of analyte that gives a response equal to three standard deviations of the blank. We calculate a 0.2-μmol methyl paraoxon/L detection limit. Some AChE-based sensors achieve lower detection limits (typically 1–10 nmol/L) because AChE irreversibly binds OPs and/or because AChE shows an extremely fast hydrolysis rate. Our current reversible sensor achieves the same level of detection as OPH-based biosensors based on potentiometry [16, 18, 19]. However, these new IPCCA OP sensors based on OPH are reversible, as shown by our use of the same sensor for replicate measurements.

Confirmation of sensing mechanism

Sharma et al. previously demonstrated a similar bimodular sensing approach for creatinine utilizing the PCCA sensing platform in which a hydroxide enzyme hydrolysis

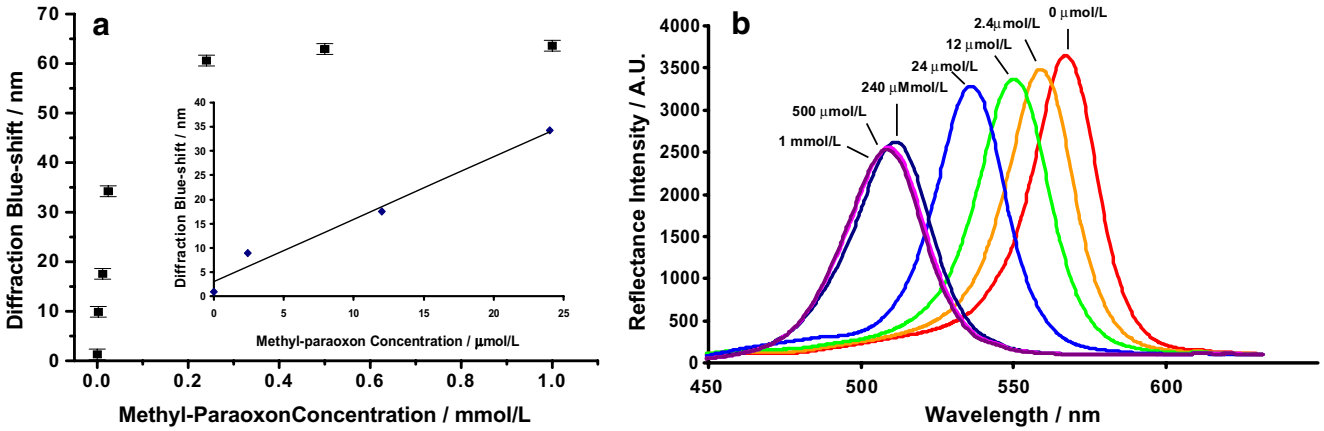

Fig. 5 **a** The PCCA diffraction wavelength as a function of methyl paraoxon concentration in BTS. *Inset* is the range (0–24 μmol methyl paraoxon/L) used to calculate the limit of detection. **b** Representative diffraction spectra of the PCCA at several methyl paraoxon concentrations. The standard error in the measurement was σ=1.1 nm for two replicates

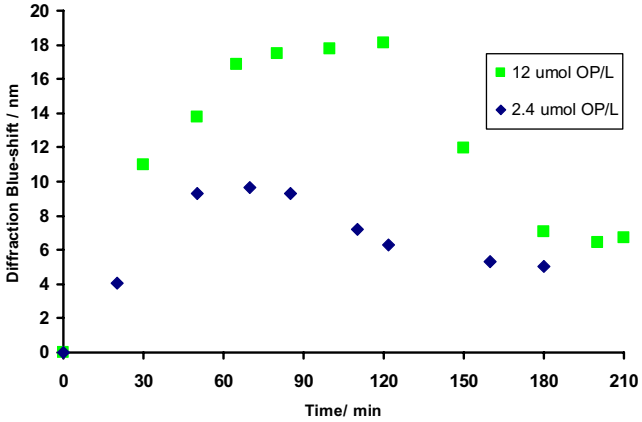

Fig. 6 Time dependence of the diffraction blueshift at two different methyl paraoxon concentrations. Steady-state is established within ~60 min. The diffraction redshifts at longer times due to depletion of the analyte

product titrated a phenol, producing a steady-state pH gradient between the interior and exterior of the hydrogel, which changed the free energy of mixing, producing a diffraction wavelength shift proportional to the analyte concentration [36]. We performed several control experiments which confirmed that our sensor was also bimodular and responded to analyte through a decrease in the free energy of mixing of the hydrogel produced by the steady-state pH gradient within the sensor, which titrates pendant phenolates.

We also tested the sensor with OP in the absence of either 3-AMP or OPH to prove that the sensing response was due to a bimodular motif. The PCCA functionalized with OPH, but the sensor lacking 3-AMP showed only a small $\Delta\lambda$=1 nm diffraction wavelength blueshift for 240 μmol methyl paraoxon/L.

A PCCA with 3-AMP and no OPH attached was also exposed to a 240-μmol methyl paraoxon/L solution. Under these conditions, the sensor actually blueshifted $\Delta\lambda$=3 nm after 60 min. This is very small compared to the normal sensing response of the IPCCA with OPH attached ($\Delta\lambda$= 62 nm). This small blueshift may result from the slow hydrolysis of methyl paraoxon in the basic solution, catalyzed by the hydrogel. The hydrolysis produces a few protons that cause the gel to shrink slightly.

We performed studies to confirm that the sensing response resulted from a steady-state response and not an equilibrium response. We monitored the absorbance of a 12-μmol methyl paraoxon/L in BTS solution exposed to an OPH-functionalized IPCCA via UV-VIS of the solution in order to calculate the rate of production of *p*-nitrophenol, which absorbs at λ= 412 nm. Using the rate of *p*-nitrophenol absorbance increase, we calculated that it would take over 3 h for the sensor to hydrolyze all of the methyl paraoxon. However, our sensor achieves full response in 50 min and thereafter remains stable for over an hour (Fig. 6). After 2 h, the sensor begins to redshift back towards the starting diffraction. We observed a similar response for 2.4 μmol methyl paraoxon/L.

This response plateau occurs because the sensor reaches a steady-state after about 1 h, where the rate of H^+ diffusion from the gel is equal to the rate of H^+ production from the OPH-mediated hydrolysis of methyl paraoxon. After 2 h, the 12 μmol methyl paraoxon/L is depleted by the enzyme, and the sensor subsequently redshifts. Our observations are consistent with the steady-state bimodular results reported by Sharma et al. [36].

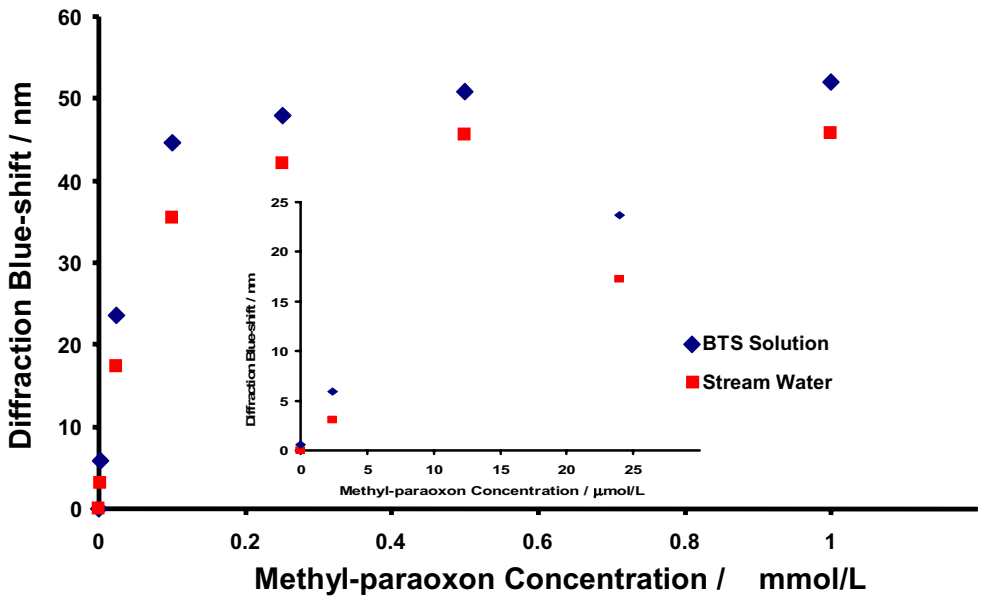

Fig. 7 PCCA OP sensor diffraction wavelength as a function of methyl paraoxon pesticide concentration in both BTS and filtered streamwater. The sensor displays a 16% smaller response in stream water compared to its response in BTS. The *inset* shows concentrations of ≤24 μmol methyl paraoxon/L

Streamwater testing

We exposed the same sensor to both methyl paraoxon in BTS as well as in a prepared streamwater sample to compare the response of the sensor to laboratory samples and to environmental samples (Fig. 7). The sensor displays a blueshift of $\Delta\lambda$=52 nm in response to 1 mmol OP/L in BTS solution, compared to a blueshift of $\Delta\lambda$=46 nm to 1 mmol OP/L in the streamwater sample. The responses in streamwater are consistently 16% smaller than in BTS at concentrations above saturation (>250 μmol OP/L).

In order to determine why the spectral window is reduced in streamwater, we titrated the streamwater sample to determine whether there was another natural buffer present, such as calcium carbonate, which would increase the effective buffer concentration and reduce the spectral window of the sensor. The streamwater did not require much base to increase the pH significantly, and no inflection point was found. The spectral window was not reduced by the presence of a natural buffer.

A possible cause of the reduction in the spectral window in real samples is the presence of other species which function as OPH inhibitors, which could cause a slower OPH turnover rate. A slower turnover rate would decrease the steady-state pH gradient, which would cause less protonation of the phenolates, which would result in a smaller diffraction blueshift.

Conclusions

We developed a sensor which is capable of determining submicromolar concentrations of the organophosphate pesticide methyl paraoxon. Organophosphorus hydrolase enzyme immobilized inside the hydrogel catalyzes the hydrolysis of methyl paraoxon, producing protons which create a steady-state pH gradient in the hydrogel. Pendant phenolates are protonated as a result of this pH gradient, causing a decrease in the free energy of mixing of the hydrogel, which shrinks the gel and blueshifts the wavelength of light diffracted by the CCA proportional to the concentration of OP in solution. The OPH-based photonic crystal sensor operates at high ionic strength and is reversible, so that it can be used as a continuous sensor for environmental sample solutions. We observe submicromolar detection limits in buffer solution. We also demonstrated that our sensor works in environmental samples by sensing methyl paraoxon in streamwater solutions. Practical application of this sensing device would involve incorporation into a monitoring device with a spectrophotometer, which could be used to detect all organophosphate species, including pesticides and nerve agents. The device could sample an environmental source and could be precalibrated to detect and quantify the amount of the organophosphate contaminant according to the wavelength of diffraction. We are currently working to increase the spectral window to span the entire visible region and to increase the sensitivity and speed of the sensor response.

Acknowledgments We gratefully acknowledge financial support from NIH grant # 2 R01 EB004132.

References

1. Hopkins EH, Hippe DJ, Frick EA, Buell GR (2000) Organophosphorus pesticide occurrence and distribution in surface and ground water of the United States, 1992–97 (Open File Report 00-187) US Geological Survey, Denver, CO
2. Burtis CA, Ashwood ER (eds) (1999) Cholinesterases. In: Tietz textbook of clinical chemistry, 3rd edn. WB Saunders, Philadelphia, PA, pp 708–711, 939–940
3. Radic Z, Pickering NA, Vellom DC, Camp S, Taylor P (1993) Biochem 32:12074
4. Dziri L, Boussaad S, Tao N, Leblanc RM (1998) Langmuir 14: 4853
5. Zaugg SD, Sandstrom MW, Smith SG, Fehlberg KM (1995) Determination of pesticides in water by C-18 solid phase extraction and capillary column gas chromatography/mass spectrometry with selected-ion monitoring (Open File Report 95-181). US Geological Survey, Denver, CO
6. Agency for Toxic Substances and Disease Registry (ATSDR) (2001) Toxicological profile for methyl parathion: update. US Department of Health and Human Services, Public Health Service, Atlanta, GA
7. Marx S, Zaltsman A, Turyan I, Mandler D (2004) Anal Chem 76:120
8. Leon-Gonzalez ME, Townshend A (1990) Anal Chim Acta 236:267
9. Constantine C, Mello SV, Dupont A, Cao X, Santos D, Oliveira ON, Strixino FT, Pereira EC, Cheng T, Defrank JJ, Leblanc RM (2003) J Am Chem Soc 125:1805
10. Mello SV, Mabrouki M, Cao X, Leblanc RM, Cheng T, Defrank JJ (2003) Biomacromolecules 4:968
11. Sacks V, Eshkenazi I, Neufeld T, Dosoretz C, Rishpon J (2000) Anal Chem 72:2055
12. Halamek J, Pribyl J, Makower A, Skladal P, Scheller FW (2005) Anal Bioanal Chem 382:1904
13. Walker JP, Asher SA (2005) Anal Chem 77:1596
14. Lai K, Dave KL, Wild JR (1994) J Biol Chem 24:16579
15. Donarski WJ, Dumas DP, Heitmeyer DP, Lewis VE, Raushel FM (1989) Biochem 28:4650
16. Mulchandani P, Mulchandani A, Kaneva I, Chen W (1999) Biosens Bioelectron 14:77
17. Cho CM, Mulchandani A, Chen W (2004) Appl Environ Microbiol 70:4681
18. Rogers KR, Wang Y, Mulchandani A, Mulchandani P, Chen W (1999) Biotechnol Prog 15:517
19. Rainina E, Efremenco E, Varfolomeyev S, Simonian AL, Wild JR (1996) Biosens Bioelectron 11:991
20. Mulchandani A, Mulchandani P, Chen W, Wang J, Chen L (1999) Anal Chem 71:2246
21. Mulchandani P, Chen W, Mulchandani A (2001) Environ Sci Technol 35:2562
22. Lei Y, Mulchandani P, Wang J, Chen W, Mulchandani A (2005) Environ Sci Technol 39:8853

23. Lei Y, Mulchandani P, Chen W, Mulchandani A (2005) J Agric Food Chem 53:524
24. LeJeune K, Wild JR, Russell AJ (1998) Nature 395:27
25. DeFrank JJ, Beaudry WT, Cheng T, Harvey SP, Stroup AN, Szafraniec LL (1993) Chem Bio Interact 87:141
26. Asher SA, Flaugh PL, Washinger G (1986) Spectroscopy 1:26
27. Carlson RJ, Asher SA (1984) Appl Spectrosc 38:297
28. Weissman JM, Sunkara HB, Tse AS, Asher SA (1996) Science 274:959
29. Reese CE, Guerrero CD, Weissmann JM, Lee K, Asher SA (2000) J Colloid Interf Sci 232:76
30. Flaugh PL, O'Donnell SE, Asher SA (1984) Appl Spectrosc 38:847
31. Rundquist PA, Photinos P, Jagannathan S, Asher SA (1989) J Chem Phys 91:4932
32. Asher SA, Holtz J, Liu L, Wu Z (1994) J Am Chem Soc 116:4997
33. Holtz JH, Asher SA (1997) Nature 389:829
34. Holtz JH, Holtz JS, Munro CH, Asher SA (1998) Anal Chem 70:780
35. Asher SA, Holtz JH, Weissman JM, Pan G (1998) MRS Bull (October) 44
36. Sharma AC, Jana T, Kesavamoorthy R, Shi L, Virji MA, Finegold DN, Asher SA (2004) J Am Chem Soc 126:2971
37. Flory PJ (1953) Principles of polymer chemistry. Cornell University Press, Ithaca, NY
38. Lybradyn, Inc. (2006) GS-10 OPH product specifications. Lybradyn, Inc., Oak Brook, IL
39. White BJ, Harmon HJ (2005) Biosens Bioelectron 20:1977
40. Dean JA (ed) (1999) Lange's handbook of chemistry, 15th edn. McGraw-Hill, New York